

A new absorption based CO₂ sensor based on Schiff base doped ethyl cellulose

Sevinç Zehra TOPAL^{1,*}, Kadriye ERTEKİN², Berrin YENİĞÜL¹,
Ayşe ERÇAĞ³

¹*Department of Chemistry, Faculty of Sciences, Ege University,
35040, Bornova, İzmir-TURKEY
e-mail: sevinczyildiz@gmail.com*

²*Department of Chemistry, Faculty of Arts and Sciences, Dokuz Eylül University,
35160, Buca, İzmir-TURKEY*

³*Department of Chemistry, Engineering Faculty, İstanbul University,
34320, Avcılar, İstanbul-TURKEY*

Received: 03.07.2010

This paper reports absorption-based CO₂ sensing of the pH-active Schiff base 2-[(2-hydroxymethylphenylimino) methyl]-5-bromo-phenol (SB) in an ethyl cellulose (EC) matrix with and without Teflon coating. The CO₂ sensitivity of the SB dye in the EC matrix was evaluated in the presence of nonadecafluorodecanoic acid and tetrabutyl ammonium hydroxide. When exposed to CO₂, the sensing films exhibited 76% of overall relative signal change and responded to CO₂ over a wide range: 1%-100 % (v/v). However, the slope of the spectral response between 1% and 5% (v/v) is more significant. The response time (τ_{90}) was 15 s, and limit of detection (LOD) was 0.3% (v/v) CO₂. The stability of SB in the EC matrix was excellent, and when stored in the ambient air of the laboratory there was no significant drift in signal intensity after 6 months. Our stability tests are still in progress.

Key Words: Absorbance, carbon dioxide, CO₂, gas sensor, Schiff base

Introduction

The continuous and accurate monitoring of CO₂ levels in the atmosphere is of great importance due to the threat of global warming. Traditionally, gaseous carbon dioxide has been assayed via infrared absorptiometry,

*Corresponding author

electrochemical Severinghouse electrode, and optical sensors. Recently, new optical sensors especially the absorption- or fluorescence-based types have attracted much attention. Most of the optical sensing schemes for the detection of carbon dioxide rely on the intensity change in the absorbance or fluorescence of an immobilized dye at a single wavelength. Such systems have some inherent drawbacks. In particular, they are disturbed by changes arising from photo bleaching or leaching. Among them, the fluorescent-based ones are more sensitive, but they are influenced by fluctuations in the light-source intensities. The ratiometric processing of the signal intensities is a desired feature in terms of practical applications since the self-calibrating ratiometric signal is mostly independent of chromophore concentration.

The pH-sensitive fluorescent indicator 1-hydroxypyrene-3,6,8-trisulfonate (HPTS) exhibits emission based ratiometric response to CO₂ and has been exploited many times in emission based sensing devices.¹⁻¹⁷ Neurauter and coworkers exploited ruthenium(II)-4,4'-diphenyl-2,2'-bipyridyl dye as luminescent donor and thymol blue (a common pH indicator) as acceptor.¹⁸ They measured CO₂ levels in the concentration range of 0-3000 Pa in an ethyl cellulose (EC) matrix.

Bromothymol blue (BTB) and thymol blue (TB) are indicators often used in absorption-based CO₂ optical sensor design. Oter et al. reported a new optical CO₂ sensor based on ion-couple of bromothymol blue/tetraoctylammonium in room temperature ionic liquids (RTILs). The detection limits were 1.4% (v/v) for gaseous CO₂ and 10⁻⁶ M HCO₃⁻ for dissolved CO₂.¹⁹ Lu and coworkers presented a sensor system suitable for monitoring changes in *p*CO₂ in surface seawater or in the atmosphere. The sensor has a response time of 2 min at the 95% equilibrium value and a measurement precision of 0.26%-0.37% in the range 200-800 μatm *p*CO₂.²⁰ An optical CO₂ sensor based on overlay of the CO₂-induced absorbance change in α-naphtholphthalein with the fluorescence of tetraphenylporphyrin using ratiometric approach was designed by Amao and coworkers. They obtained 53.9% signal change from N₂ to CO₂.²¹ Muda et al. reported a novel optical-fiber-based sensor for measurement of CO₂ gas emission concentrations in the exhaust system of a motor vehicle. The sensing principle is based on open-path direct absorption spectroscopy in the mid-infrared range. The sensor has demonstrated operation over the range of 1%-12 % (v/v) CO₂.²² CO₂ selective films designed for clinical application based on the co-incorporation of different phenol dyes, naphtholphthalein, naphthol blue black, and calmagite with tetraoctylammonium hydroxide into metaloxide nanoporous matrices were described by Sanchez and coworkers. The sensing films responded to absorption based on CO₂ concentrations in the gas phase between 0.25% and 40% CO₂.²³ The CO₂ sensing both in gaseous and dissolved forms is still an important issue among analytical chemists. In most of the sensitive emission-based sensors short storage lifetime appears to be a problem. Others may suffer from low relative signal changes, interference effects of other ionic species, or limited working ranges.

This paper presents the absorption-based CO₂ response of the Schiff base (SB) 2-[(2-hydroxymethylphenyl)limino) methyl]-5-bromo-phenol EC matrix in the presence of additives of nonadecafluorodecanoic acid and tetrabutyl ammonium hydroxide. The absorption based stable signal of the proposed sensor is compatible with most of the currently available ones in terms of signal stability and storage lifetime. Addition of the nonadecafluorodecanoic is expected to make a contribution to analyte solubility within the polymer matrix.

Experimental

Instruments

The absorption spectra of the solutions and sensor films were measured by Shimadzu 1601 UV-Visible spectrophotometer. The pH values of the solutions were checked using a digital pH meter (WTW) calibrated with standard buffer solutions from Merck. Different CO₂ standards [0%-100% (v/v)] in a gas stream were produced by controlling the flow rates of CO₂ and nitrogen gases entering in a gas diluter Sonimix 7000A gas-blending system. The total pressure and the output flow rate of the gas mixture were maintained at 760 Torr and 250 mL min⁻¹, respectively. Gas mixtures were introduced into the cuvette containing the sensing films via a diffuser needle under ambient conditions either directly or after humidification of the gas by bubbling through water at 25 °C. All the experiments were carried out at room temperature: 25 ± 1 °C.

Materials

The SB 2-[(2-hydroxymethylphenylimino) methyl]-5-bromo-phenol was synthesized from 5-bromo salicylaldehyde and 2-aminobenzyl alcohol according to the method we reported previously.²⁴ 5-Bromo salicylaldehyde, 2-aminobenzyl alcohol, dichloromethane (DCM), ethanol (EtOH), tetrahydrofuran (THF), toluene, and tetrabutylammonium hydroxide (TBAOH in isopropanol) were purchased from Aldrich and used without purification. The perfluorochemical (PFC) nonadecaperfluorodecanoic acid [CF₃(CF₂)₈CO₂H], potassium tetrakis-(4-chlorophenyl) borate (PTCPB), and the plasticizer bis-(2-ethylhexyl)phtalate (DOP) were purchased from Fluka. Ethyl cellulose (with an ethoxy content of 46%) was purchased from Aldrich. Teflon AF (type 1600) and the polyester support (Mylar[®] type) were purchased from DuPont polymers. Buffer solutions were prepared with disodium hydrogen phosphate/sodium hydroxide for pH 12.0, sodium dihydrogen phosphate/sodium hydroxide for pH 7.0, and phosphoric acid/sodium hydroxide for pH 2.0. Millipore pure water was used throughout the studies. Carbon dioxide and nitrogen of 99.99% purity were obtained from Karbogaz Company, İzmir, Turkey.

Polymer film preparation protocols

The optode membranes were prepared to contain different contents. Cocktail 1 (C-1) contains 100 mg of EC, 200 mg of DOP, 2.0 mg of SB dye, 2 mg of PTCPB, and 1.5 mL of THF. The other compositions contain additives of 1 mg of PFC, CF₃(CF₂)₈CO₂H, and/or 100 μL of 1.00 M TBAOH and are described in Table 1. The resulting cocktails were spread onto a 125 μm polyester support (Mylar[®] type) in order to obtain the sensing films. Film thickness of sensing films was measured as 5.38 μm with a Tencor Alpha Step 500 Prophyrometer. Each sensing film was cut to 1.2 × 3.0 cm size. Some of the films were covered non-viscous Teflon solution by spreading technique.

Results and discussion

Photocharacterization of the Schiff base (SB) and sensing properties

Spectral characterization of SB dye was performed in conventional solvents and in EC matrix by means of absorption spectroscopy. Chemical structure and absorption spectra of SB dye in the absence and presence

of TBAOH are shown in Figure 1. UV-Vis related data are given in Table 2. In immobilized form molar absorptivity (ϵ) of the SB was enhanced about 5-fold with respect to ϵ values calculated in the solvents. In the presence of TBAOH, absorption wavelength maxima of SB in the solvent were shifted to red. As stated by Kessler and Wolfbeis, depending on the nature of the interaction between the dye and its microenvironment, the dye may undergo changes in molar absorptivities.²⁵

Table 1. Compositions of CO₂ sensing cocktails based on EC doped SB dye.

Cocktail no.	Additive
C-1	-
C-2	PFC (1 mg)
C-3	TBAOH (100 μ L)
C-4	PFC (1 mg) + TBAOH(100 μ L)

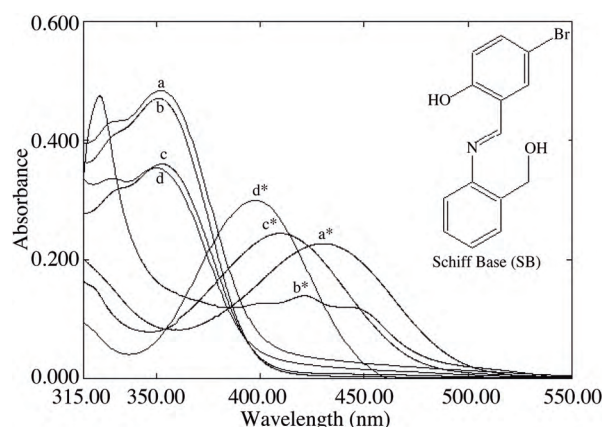


Figure 1. Chemical structure of the Schiff base, SB dye, and its absorption spectra in the absence and presence* of TBAOH in the solvents: (a) THF, (b) DCM, (c) Toluene-EtOH, (d) EtOH.

Table 2. UV-Vis spectra related data of the Schiff base in the solvents of EtOH, DCM, To:EtOH (80:20), THF, and in solid matrix of EC.

Acidity	Solvents/Matrix	λ_{\max} (nm)	ϵ_{\max} (10^4)
Schiff base in acidic/neutral media	EtOH	352	1.1
	THF	351	1.0
	DCM	353	1.0
	To:EtOH	350	1.1
	EC (C-1)	356	5.0
Schiff base in basic media	EtOH	398	8.6
	THF	422	1.1
	DCM	430	1.1
	To:EtOH	410	1.1
	EC (C-4)	415	2.2

Because of the proposed SB dye meets the requirement of exhibiting relatively high molar absorptivity and long-term stability with CO₂ sensing, the chosen SB is suitable for CO₂ sensing applications.

pK_a measurements

Indicators that have pK_a values between 6.8 and 10.0 are essential for sensitive pCO₂ optodes; this is why the determination of the dissociation constant (pK_a) of dye in EC matrix is important. The acidity constants of SB were calculated for the C-1 composition without acidic or basic additives. Figure 2 shows the absorption-based response of EC doped SB in the pH range of 5.50-11.50. The absorption spectra of SB dye shifted from 338 to 372 nm with the deprotonation process. The plot of normalized absorbance (A/A_o) versus measured pH values in EC matrix was shown as an inset in Figure 2. Two different pK_a values were estimated at 6.8 and 9.7 from the midpoints of the plot. Moreover, pK_a values were also calculated from the non-linear fitting algorithm of Gauss-Newton-Marquart:

$$pK_a = pH + \log[(I_b - I_x)/(I_x - I_a)] \quad (1)$$

where I_a and I_b are the absorption signal intensities of the dye in their acid and conjugate base form and I_x is the intensity at a pH approximate to the pK_a.²⁶ The distinct pK_a values were 6.8 ± 0.1 and 9.6 ± 0.1 (n = 3).

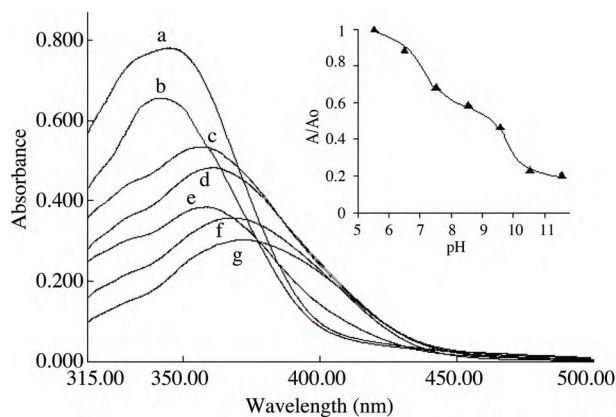


Figure 2. Absorption-based spectral response of C-1 in the pH range of 5.5- 11.5 in phosphate buffer. pH: (a) 5.5, (b) 6.5, (c) 7.5, (d) 8.5, (e) 9.5, (f) 10.5, (g) 11.5, Inset: The plot of normalized absorbance (A/A_o) versus measured pH values in EC matrix.

When SB dye is doped into plasticized EC together with the anionic additive potassium tetrakis-(4-chlorophenyl) borate (PTCPB), it becomes reversibly working H⁺ selective probes. The response mechanism of such systems depends on ion-exchange of proton and anionic additive PTCPB between the solution and organic (film) phase.

Figure 3-I and 3-II show the possible protonation mechanism of the basic nitrogen atom of the SB and the following charge delocalization on the phenolic ring, and the possible deprotonation mechanism in alkaline media, respectively.

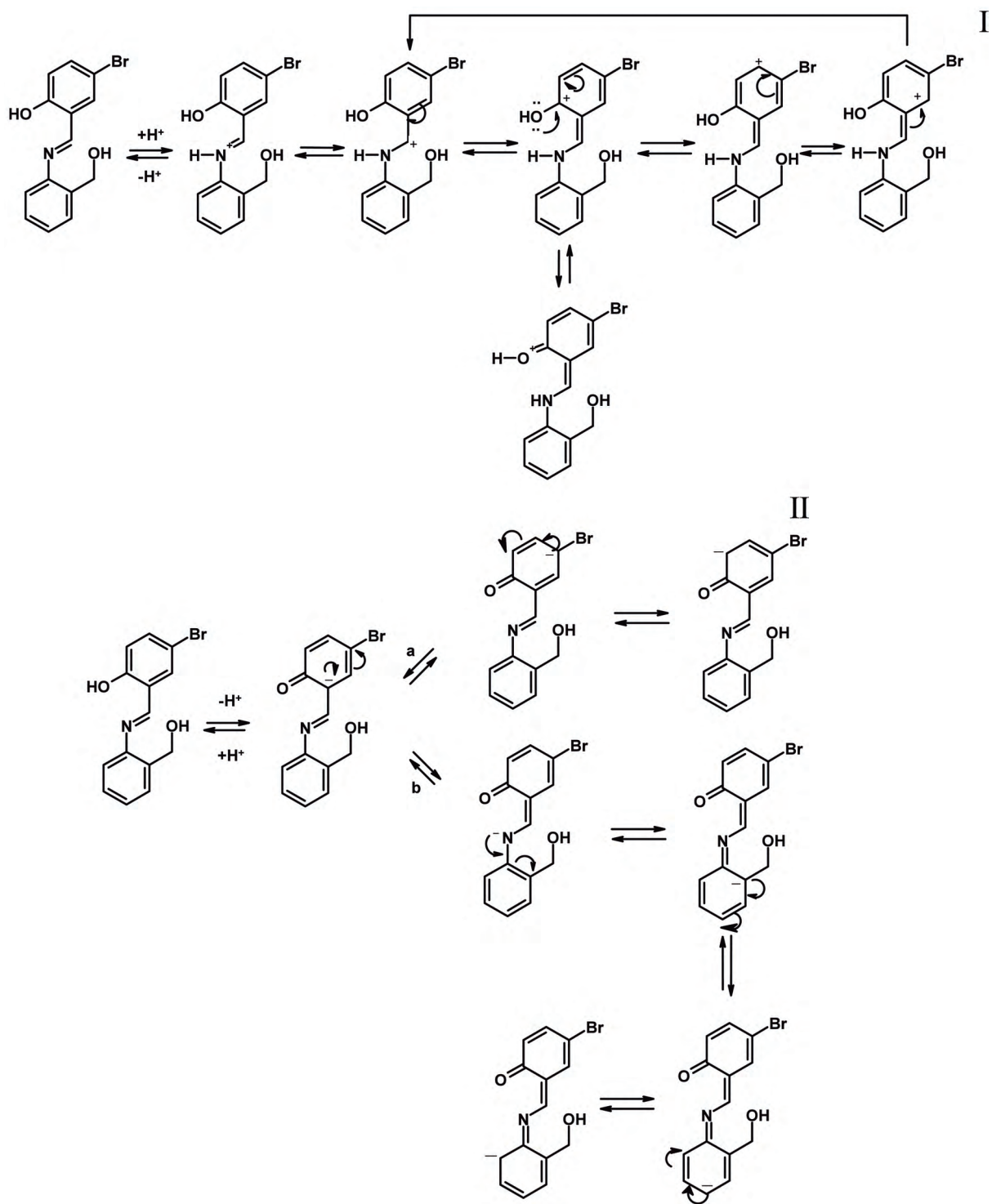


Figure 3. [I] Protonation of the Schiff base from nitrogen atom and following positive charge delocalization. [II] Deprotonation mechanism of the Schiff base in alkaline media; deprotonation from phenol ring and following negative charge delocalization. -a: favored, -b: favored but unproductive deprotonation route.

CO₂ sensing studies

In such designs, the principle of CO₂ sensing is based on use of a pH indicator dye whose absorption is modified in the presence of CO₂. The pH indicator dye was protonated with carbonic acid formed from dissolved CO₂ in water. Absorption-based sensing is based on 2 processes, the first being the diffusion of CO₂ through the membrane into the sensing region and the second being the reaction of the gas with SB.

CO₂ response of SB films prepared in different compositions (C-1; C-4) was investigated in detail. Figure 4 reveals the absorption spectra of the dye in different matrix compositions. In the case of C-1 and C-2, the dye is in acidic form. However, with compositions of C-3 and C-4 the dye is basic form due to the presence of the quaternary ammonium base TBAOH. In order to provide functionality of the sensor, the dye should be in basic form. Figure 5 reveals the response of the sensing slides to CO₂ in the presence and absence of PFC. The attained relative signal changes for the films C-3 and C-4 to 100% (v/v) CO₂ were 72% and 76%, respectively. In agreement with literature, PFC doped composition (C-4) exhibited 4% higher relative signal change due to the better carbon dioxide solubility.^{6,12} Finally, the best response was observed for C-4 film, which contains both additives in the same composition, TBAOH, a phase transfer agent, and PFC, a carbon dioxide carrier. In order to avoid the interference effects of other acidogenic species, we coated some compositions with Teflon. The exploited Teflon membrane is permeable for gaseous but impermeable for ionic species.

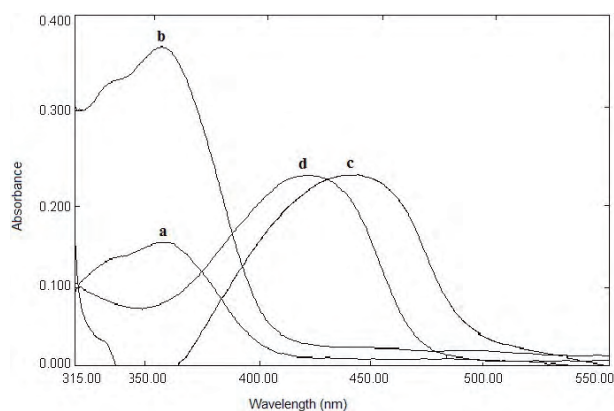


Figure 4. Absorption spectra of the Schiff base in different cocktail compositions: (a) C-1 (b) C-2 (c) C-3 (d) C-4.

Figure 6-I and 6-II show the absorption-based sensor response of the Teflon-free and Teflon-coated C-4 films upon exposure to CO₂ in the range of 0%-100% (v/v). In the Teflon-free thin films absorption bands of the dye appeared at 356 and 409 nm and an isobestic point was observed at 374 nm. In the Teflon-coated films, the long wavelength absorption band was 10 nm redshifted and appeared at 419. The isobestic point was also slightly redshifted and was observed at 378 nm. Relative signal changes in the Teflon-free and Teflon-coated membranes were 76% and 68%, respectively.

The existence of an isobestic point allows the ratiometric measurements. In ratiometric signal processing, (A_{409}/A_{356}) and (A_{419}/A_{356}) were used to plot the calibration graph of the sensing C-4 film, where A_{409} and A_{356} represent absorbance values at the cited wavelengths (see Figure 7). The proposed sensor slides exhibited an absorption-based response in a large CO₂ concentration range with reliable ratiometric data.

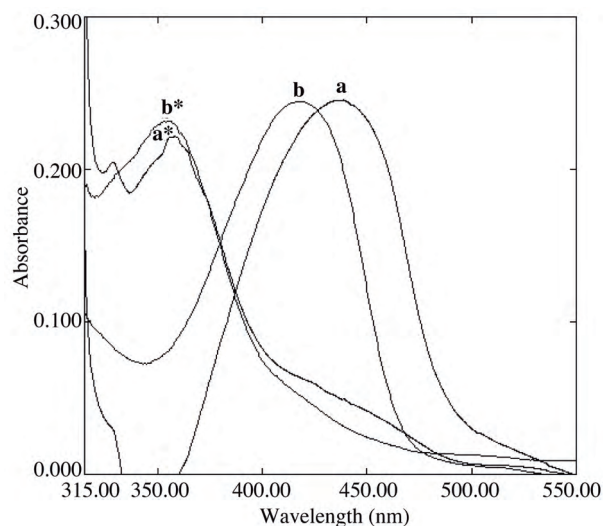


Figure 5. Absorption spectra of C-3 and C-4 films before and after* exposure to 100% CO₂: (a) C-3 (a*) C-3 (b) C-4 (b*) C-4.

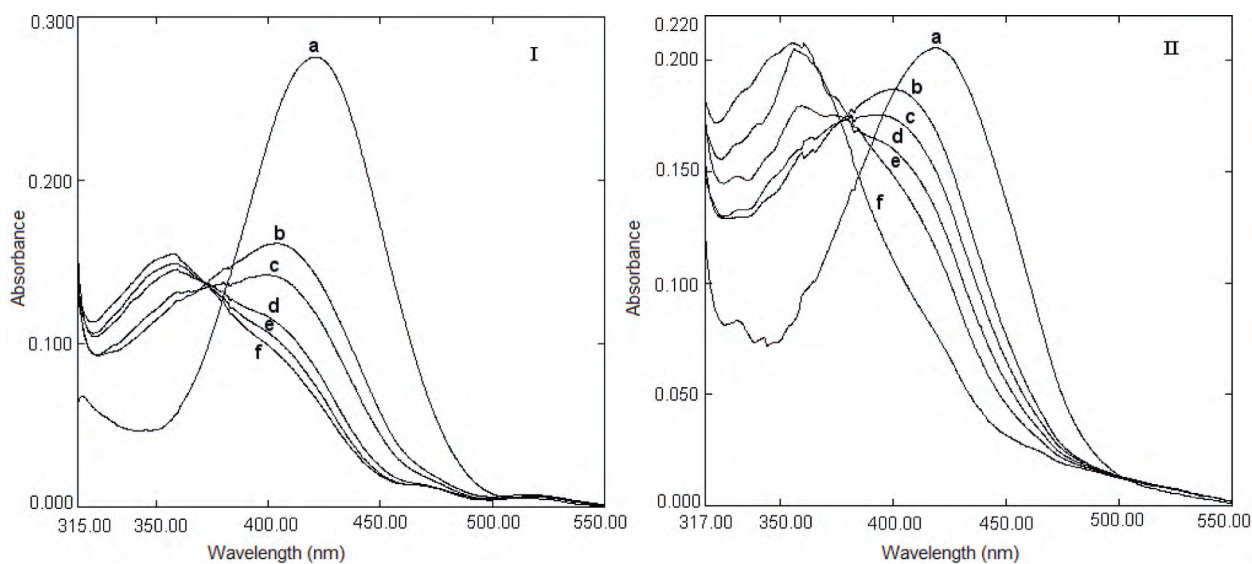


Figure 6. Absorption spectra of C-4 films after exposure to % (v/v) CO₂: (a) 0 (b) 20 (c) 40 (d) 60 (e) 80 (f) 100; I: Teflon-free, II: Teflon-coated membranes.

The absorption-based spectral response of C-4 after exposure to 0%-20 % (v/v) CO₂ was investigated in detail, because the sensing films exhibited remarkably high relative signal change to 0%-20% (v/v) CO₂ (see Figure 8). The sensor membrane prepared from C-4 exhibited a linear response to CO₂ in the concentration range of 0%-5% (v/v) CO₂ with a correlation coefficient of $R^2 = 0.9536$ (see inset of Figure 8).

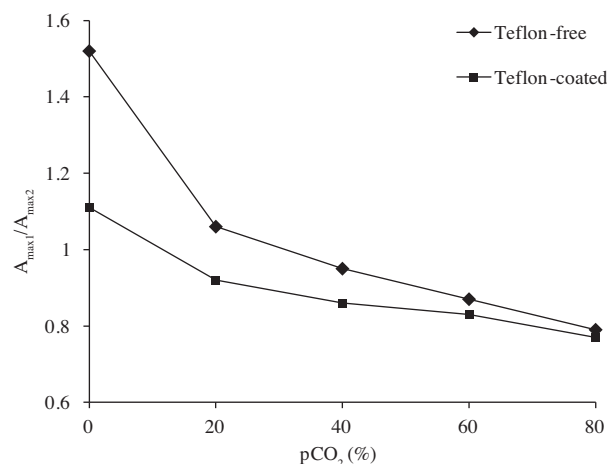


Figure 7. Non-linearized ratiometric calibration plot of C-4 films.

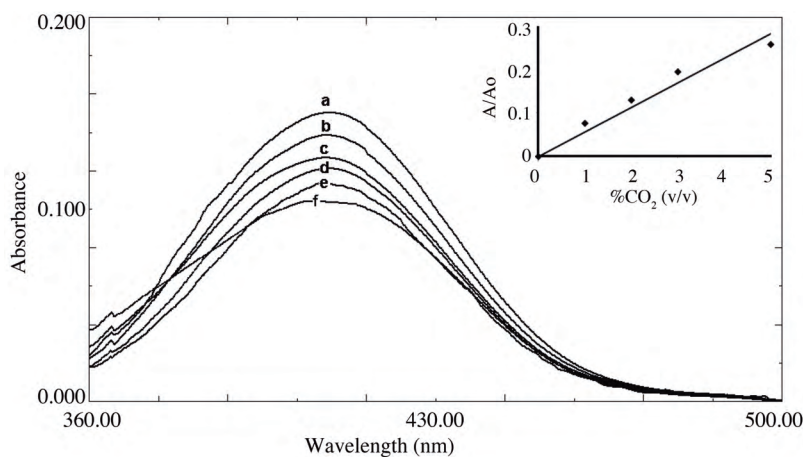


Figure 8. Absorption spectra of C-4 films after exposure to 0%-20% CO₂ (v/v) concentrations: (a) 0 (b) 1 (c) 2 (d) 3 (e) 5 (f) 20. Inset: Linearized calibration curve of C-4 film after exposure to 0%-5% CO₂.

When the results shown in Figures 7 and 8 are considered together it can be concluded that the intensity-based sensor response is different in terms of slope in the concentration range of 0%-5% and 20%-80% (v/v) CO₂. It should be noted that the isobestic point does not seem to be valid for low CO₂ concentrations.

Response, recovery, and stability characteristics

Figure 9 illustrates the response characteristics of C-4 film in an alternating atmosphere of 20% (v/v) CO₂ and 100% (v/v) N₂. After the second measurement no drift was observed in the following cycles.

Response time is the time it took for the sensor to detect 90% of the change in absorption signal. In our case the response time of the sensor (τ_{90}) was 15 s when switching from N₂ to CO₂ and 290 s when switching from CO₂ to N₂ from the measurements performed in the “time-based mode”. The reported response time

is compatible with some of the currently available sensors. However, response and regeneration times can be improved by decreasing the film thickness, which is an important parameter of response time.²⁷

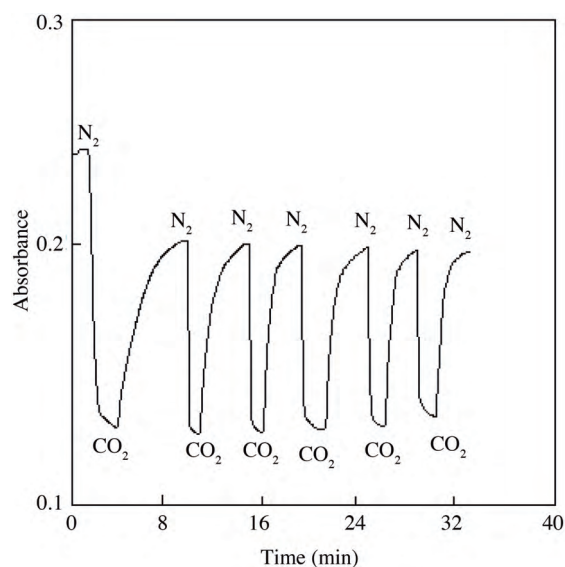


Figure 9. Response of sensor composition; C-4 at 415 nm in an alternating atmosphere of 20% CO₂ and 100% N₂ (v/v).

The limit of detection (giving a signal equal to the blank signal, plus 3 times the standard deviation of the blank) was found to be 0.3% (v/v) for gaseous CO₂.

The photostability of the SB dye was tested and evaluated in solid matrix of EC under a xenon-arc lamp and solar radiation. The short-term photostability of SB was measured in time-based mode over 1 h (see Figure 10). In all the employed media, SB exhibited excellent short-term photostability. Long-term stabilities of the sensing films were tested over 6 months. It was found to be nearly the same with an intensity loss of only 1%-2% when the thin films were stored in ambient air. Our stability tests are still in progress.

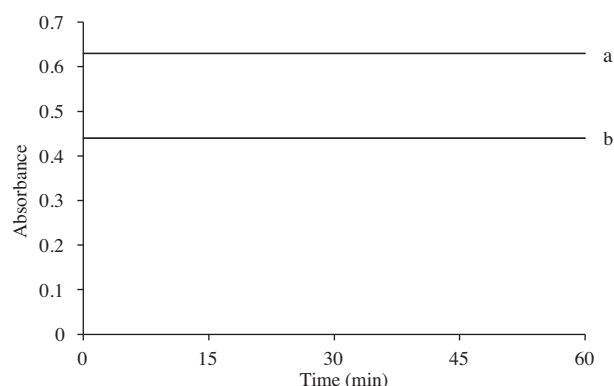


Figure 10. Photostability test results of the ratiometric Schiff base: after exposure to light for 1 h of monitoring in different media: (a) EtOH b) sensor composition of C-4.

Cross-sensitivity to metal cations and other gases

The cross-sensitivity of the Teflon-free C-1 composition to polyvalent metal ions was investigated by exposure to 10⁻³ M solutions of Zn²⁺, Hg⁺, Sn²⁺, Ca²⁺, Bi³⁺, Ni²⁺, Co²⁺, Cu²⁺, Pb²⁺, Al³⁺, Cr³⁺, Mn²⁺, and Fe³⁺ in acetic acid/acetate buffered solutions at pH 5.0. For common polyvalent metal ions except Zn ion, relative errors of less than 5% were obtained, which was considered tolerable. The response of SB dye to oxygen gas was also investigated in the same concentration range as CO₂. The SB dye did not respond to oxygen gas.

The Teflon-free C-1 films responded to Zn²⁺ ions in the direction of signal decrease. In the case of the presence of Zn²⁺ ions, Teflon-coated films should be used. It should be noted that spectroscopic responses to metal ions are dependent on many factors, including pH, temperature, viscosity, and the presence of other ions.

Conclusion

This paper presents an absorption-based optical CO₂ sensor employing a SB, 2-[(2-hydroxymethylphenylimino)methyl]-5-bromo-phenol, in EC matrix in the presence of TBAOH and PFC. The proposed sensor exhibited a wide dynamic working range (1.0%-80% (v/v) CO₂), short response time (15 s), remarkably high relative signal change (76%), long-term stability (over 6 months), and high selectivity. Moreover, SB dye exhibited an isobestic point, allowing ratiometric measurements. The sensor response should be evaluated in 2 different concentration ranges. The stable response in the concentration range of 1%-5% (v/v) may have potential use for environmental monitoring studies and clinical purposes.

Acknowledgement

Funding for this research was provided by The Scientific and Technological Research Council of Turkey (TÜBİTAK) (Project number 104M268). Sevinç Zehra Topal is also grateful to TÜBİTAK-BİDEB-2211 for support to her PhD studies. We also thank Prof. Dr Yavuz Ergün (Dokuz Eylül University) for his critical comments.

References

1. Weigl, B. H.; Wolfbeis, O. S. *Anal. Chim. Acta* **1995**, *302*, 249-254.
2. Von Bultzingslowen, C.; McEvoy, K. A.; McDonagh, C.; MacCraith, B. D.; Klimant, I.; Krause, C.; Wolfbeis, O. S. *Analyst* **2002**, *127*, 1478-1483.
3. Wolfbeis, O. S.; Kovacs, B.; Goswami, K.; Klainer, S. M. *Microchim. Acta* **1998**, *129*, 181-188.
4. Malins, C.; MacCraith, B. D. *Analyst* **1998**, *123*, 2373-2376.
5. Neurauter, G.; Klimant, I.; Wolfbeis, O. S. *Fresenius J. Anal. Chem.* **2000**, *366*, 481-487.
6. Ertekin, K.; Klimant, I.; Neurauter, G.; Wolfbeis, O. S. *Talanta* **2003**, *59*, 261-267.
7. Yafuso, M.; Suzuki, J. K. *US Patent* **1989**, 4824789.
8. Alderete, J. E.; Olstein, A. D.; Furlong, S. C. *US Patent* **1998**, 5714121.

9. Adrian, W.; Mark, B. S. *US Patent* **2002**, 6338822.
10. Furlong, S. C. *US Patent* **1997**, 5672515.
11. Burke S. C.; Markey A.; Nooney R. I.; Byrne P.; McDonagh C. *Sens. Actuators B* **2006**, *119*, 288-294.
12. Oter, O.; Ertekin, K.; Topkaya, D.; Alp, S. *Anal. Bioanal. Chem.* **2006**, *386*, 1225-1234.
13. Chu, C.; Lo, Y. *Sens. Actuators B* **2009**, *143*, 205-210.
14. De Vargas-Sansalvador, I. M. P.; Carvajal, M. A.; Roldan-Munoz, O. M.; Banqueri, J.; Fernandez-Ramos, M. D.; Capitan-Vallvey, L. F. *Anal. Chim. Acta* **2009**, *655*, 66-74.
15. Chu, C.; Lo, Y. *Sens. Actuators B* **2008**, *129*, 120-125.
16. Schroeder, C. R.; Neurauder, G.; Klimant, I. *Microchim. Acta* **2007**, *158*, 205-218.
17. Müller, B.; Hauser, P. C. *Analyst* **1996**, *121*, 339-343.
18. Neurauder, G.; Klimant, I.; Wolfbeis, O. S. *Anal. Chim. Acta* **1999**, *382*, 67-75.
19. Oter, O.; Ertekin, K.; Topkaya, D.; Alp, S. *Sens. Actuators B* **2006**, *117*, 295-301.
20. Lu, Z.; Dai, M.; Xu, K.; Chen, J.; Liao, Y. *Talanta* **2008**, *76*, 353-359.
21. Amao, Y.; Nakamura, N. *Sens. Actuators B* **2004**, *100*, 347-351.
22. Muda, R.; Dooly, G.; Clifford, J.; Mulrooney, J.; Flavia, G.; Merlone-Borla, E.; Chambers, P.; Fitzpatrick, C.; Lewis, E. *J. Opt. A: Pure Appl. Opt.* **2009**, *11*, 054013-054019.
23. Fernandez-Sanchez, J. F.; Cannas, R.; Spichiger, S.; Steiger, R.; Spichiger-Keller, U. E. *Sens. Actuators B* **2007**, *128*, 145-153.
24. Kaya, I.; Erçağ, A.; Çulhaoğlu, S. *Turk J Chem* **2007**, *31*, 55-63.
25. Kessler, M. A.; Wolfbeis, O. S. *Spectrochim. Acta A* **1991**, *47*, 187-192.
26. Werner, T.; Wolfbeis, O. S. *Fresenius J. Anal. Chem.* **1993**, *346*, 564-568.
27. Stangelmayer, A.; Klimant, I.; Wolfbeis, O. S. *Fresenius J Anal Chem* **1998**, *362*, 73-76.